Simulation of liquid penetration in paper

J. Hyväluoma, P. Raiskinmäki, A. Jäsberg, A. Koponen, M. Kataja, and J. Timonen
Department of Physics, University of Jyväskylä, FI-40014 Jyväskylä, Finland
(Received 25 October 2005; published 15 March 2006)

Capillary penetration of a wetting liquid in a microtomographic image of paper board, whose linear dimension was close to the average length of wood fibers, was simulated by the lattice-Boltzmann method. In spite of the size of the system not being large with respect to the size of structural inhomogeneities in the sample, for unidirectional penetration the simulated behavior was described well by that of the Lucas-Washburn equation, while for radial penetration a radial capillary equation described the behavior. In both cases the average penetration depth of the liquid front as a function of time followed a power law over many orders of magnitude. Capillary penetration of small droplets of liquid was also simulated in the same three-dimensional image of paper. In this case the simulation results could be described by a generalized form of the radial-penetration equation.

DOI: 10.1103/PhysRevE.73.036705 PACS number(s): 47.11.−j, 47.56.+r, 81.05.Rm

I. INTRODUCTION

Penetration of fluid into small pores of a solid material is a common phenomenon in nature, and it also appears in many technological processes. Examples of such penetration range from water transport in plants to applications in the printing and textile industries. The basic equation used to describe capillary penetration was introduced by Lucas and Washburn almost a century ago [1,2], but its validity in various experimental situations is still being analyzed [3–5]. Most experiments have been carried out at length scales much larger than the structural inhomogeneities in the porous materials analyzed. Thus one of the interesting remaining questions is how well simple capillary models with grossly simplified assumptions about the pore structure can describe fluid transport in length scales close to and even below those of structural variations.

Many fascinating phenomena are related, e.g., to imbibition in which a fluid penetrates a porous medium filled by another fluid (for a recent review see, e.g., Ref. 6). Examples of these phenomena include the roughening of an interface between the two fluids [7], pinning of such an interface induced by evaporation or by random inhomogeneities [8,9], and other defect-induced effects on it [10]. A great deal of recent interest has also been devoted to propagation of the so-called precursor fronts that are formed when pores of considerably different sizes (e.g., microrougheness at pore walls) are interconnected in the medium [5,11,12].

The development of new and improvement of old techniques for fluid-flow simulations has recently opened up new possibilities in the study of complex multiphase flow phenomena such as, e.g., imbibition. One of the new methods applicable rather generally to multiphase flows is the lattice-Boltzmann (LB) method [13–16]. This method has in fact been found to be an efficient tool in simulating complex flow problems. For instance, it has been successfully used to simulate flows in porous media [17,18], multiphase flows [19–25], and suspension flows [26–30]. Particularly interesting properties of the LB method include its spatially local updating rules, which make it suitable for parallel computing [31–33], and easy handling of fluid-solid boundaries, which is advantageous when simulating flows in complex geometries.

In this work we thus use the LB method to study capillary penetration of a wetting liquid in paper board. Paper is an interesting common material for this kind of study. In spite of the fact that it has been used in many experimental studies of liquid penetration (cf. Refs. [5,34–38]), the small-scale dynamics of imbibition in paper is still largely unknown. It is not known, in particular, whether capillary models can be used to describe this dynamics as many of the simplifying assumptions behind these models are not really valid. In addition, penetration of liquid into paper is of great practical interest, not only in paper-making processes such as coating, but also in printing or when using paper as an absorbing material. We demonstrate here that results of *ab initio* LB simulations for fluid transport in length scales up to the average length of the wood fibers that mainly constitute the material are indeed in good agreement with predictions of appropriate capillary models. It is evident that similar simulations could be used to analyze related technological processes.

In these simulations paper was described by a three-dimensional (3D) reconstruction of a sample of paper board, based on high-resolution x-ray microtomography. In tomographic imaging a large number of 2D projections of the sample are collected by passing radiation through it at different angles. By Radon transformation [39] these shadowgrams are transformed into 2D cross sections for the local absorption coefficient of x rays, from which a 3D map of the absorption coefficient can be constructed [40]. By segmenting the gray-scale values that describe the fiber material, the structure of the original sample is recovered. An accurate determination of the air-fiber boundary is, however, not straightforward; see, e.g., Ref. [41]. Recent advancements in the resolution of x-ray microtomography have made tomographic reconstructions rather realistic images of materials such as paper; see, e.g., Refs. [42–44].

To begin with we review some capillary models that are relevant to the liquid-penetration problem considered here. Thereafter we briefly describe the single-component multiphase lattice-Boltzmann model used in the simulations. In

the results section three different cases are considered: unidirectional and radial penetration of liquid from an infinite liquid source and penetration of a small liquid droplet. Notice that we also consider penetration of liquid in the thickness direction of the paper sample, for which experimental results are not available. Finally we draw some conclusions based on the results reported.

II. CAPILLARY MODELS

Models that describe capillary penetration of a liquid in porous materials are usually based on expressions for a single-capillary tube. Although this is a major simplification of the actual pore structure of most porous materials, these models have often turned out to correctly describe the capillary penetration if an effective pore radius is used to characterize the material. Applying Newton's second law on a column of a viscous and incompressible liquid rising in a capillary tube and assuming that the flow is laminar and fully developed (Poiseuille flow), one easily arrives at the equation

$$\rho\left[z\frac{d^2z}{dt^2}+\frac{1}{2}\left(\frac{dz}{dt}\right)^2\right]=\frac{2\gamma\cos\theta}{a}-\frac{8\mu z}{a^2}\frac{dz}{dt}, \tag{1}$$

where z is the height of the column, a the radius of the tube, ρ the density, γ the surface tension, θ the contact angle, and μ the viscosity of the liquid. We have neglected the effect of gravity since in the simulations reported in Sec. IV we only consider situations in which gravity is not present. The classical result of Lucas [1] and Washburn [2] is obtained from Eq. (1) by neglecting the inertial terms. This leads to the Lucas-Washburn equation

$$\frac{2\gamma\cos\theta}{a}-\frac{8\mu z}{a^2}\frac{dz}{dt}=0. \tag{2}$$

This simple equation refers to a quasi-steady-state process where the driving capillary force is balanced by the viscous drag. It can be integrated, and one finds for the time evolution of the height of the liquid column the result

$$z(t)=\left(\frac{a\gamma\cos\theta}{2\mu}\right)^{1/2}t^{1/2}. \tag{3}$$

Experimental results indicate that this model can be used to describe the average large-scale time evolution of liquid penetration also in more complex capillary systems and in porous media such as paper [5,35,38].

It is also of interest to consider two-dimensional radial penetration of liquid in a porous medium. Here we concentrate on the case in which penetration takes place from an unlimited source of liquid. We derive an equation for two-dimensional radial penetration starting from Darcy's law,

$$\frac{Q}{A}=-\frac{k}{\mu}\frac{\partial P}{\partial r}, \tag{4}$$

where Q is the volumetric flow through a cross section of area A, k is the permeability of the medium, and P is the pressure. Since for the radial penetration $A=2\pi rH$, with H the thickness of the medium, integration of Eq. (4) yields

$$P_c=P(R_0)-P(R)=\frac{Q\mu}{2\pi Hk}\ln\frac{R}{R_0}, \tag{5}$$

where P_c is the capillary pressure, R the radius of the wetted area, and R_0 that of the liquid source. Using the average liquid velocity $V=dR/dt$, Eq. (5) becomes a differential equation

$$P_c=\frac{R\phi\mu}{k}\ln\left(\frac{R}{R_0}\right)\frac{dR}{dt}, \tag{6}$$

where ϕ is the porosity of the medium. This equation can also be integrated, and we find that

$$\left(\frac{R}{R_0}\right)^2\left(\ln\frac{R}{R_0}-\frac{1}{2}\right)+\frac{1}{2}=\frac{2kP_c}{\phi\mu R_0^2}t. \tag{7}$$

Capillary pressure can be written as $P_c=2\gamma\cos\theta/a$, and different models for permeability k may be used. For example, the permeability of a system that consists of capillary tubes of radius a is found to be $k=\phi a^2/24$. More sophisticated models of permeability of low-Reynolds-number flows through porous materials can be found in, e.g., Ref. [45]. However, this simple model for permeability is mostly enough for our purposes. In this case Eq. (7) takes the form

$$\left(\frac{R}{R_0}\right)^2\left(\ln\frac{R}{R_0}-\frac{1}{2}\right)+\frac{1}{2}=\frac{\gamma a\cos\theta}{6\mu R_0^2}t. \tag{8}$$

This equation resembles the one derived by Marmur for radial penetration in a single radial capillary formed between two infinite parallel plates with a cylindrical source of liquid [46]. There is, however, a different numerical constant in that case on the right-hand side of the equation. The qualitative validity of an equation of this kind for planar capillary systems was verified experimentally by Borhan and Rungta [37] and by Danino and Marmur [38]. Notice that also in these experiments, only large-scale (over a scale of tens of centimeters) dynamics was considered.

III. LATTICE-BOLTZMANN METHOD AND THE SHAN-CHEN MULTIPHASE MODEL

The lattice-Boltzmann method is a discrete kinetic-theory-based method to simulate fluid flow [14,15]. Of the several different LB methods that exist, we adopt here the one based on the simple single-relaxation-time approximation for the collision operator—i.e., the lattice Bhatnager-Gross-Krook (BGK) model [47]). This method is based on the LB equation

$$f_i(\mathbf{r}+\mathbf{c}_i,t+1)=f_i(\mathbf{r},t)+\frac{1}{\tau}[f_i^{eq}(\mathbf{r},t)-f_i(\mathbf{r},t)], \tag{9}$$

which governs the evolution of the single-particle distribution functions f_i related to discrete velocities $\mathbf{c}_i$ and the f_i^{eq} are the corresponding equilibrium distributions towards which the distribution functions are relaxed in collisions. The collision processes are characterized by a relaxation time τ. We use in our simulations the three-dimensional 19-velocity

LB model D3Q19 [48]. In this model the possible discrete velocities are zero for the rest particles, 6 velocities to the nearest-neighbor lattice nodes of a cubic lattice and 12 velocities to the next-nearest-neighbor lattice nodes. In the D3Q19 model the equilibrium distribution function is of the form

$$f_i^{eq}(\mathbf{r},t) = \rho t_i\left(1 + \frac{1}{c_s^2}(\mathbf{c}_i \cdot \mathbf{u}) + \frac{1}{2c_s^4}(\mathbf{c}_i \cdot \mathbf{u})^2 - \frac{1}{2c_s^2}\mathbf{u}^2\right), \tag{10}$$

where the weight factor t_i has a value 1/2, 1/18, and 1/36 for the rest particles and for the particles moving to nearest and next-nearest neighbors, respectively. The speed of sound in this model is $c_s = 1/\sqrt{3}$, and the kinematic viscosity is $\nu = (2\tau - 1)/6$. Mass and momentum densities are determined from moments of the distribution functions such that, respectively,

$$\rho(\mathbf{r},t) = \sum_i f_i(\mathbf{r},t) \tag{11}$$

and

$$\rho(\mathbf{r},t)\mathbf{u}(\mathbf{r},t) = \sum_i f_i(\mathbf{r},t)\mathbf{c}_i. \tag{12}$$

The no-slip boundary condition between the fluid and solid phases is realized with the bounce-back rule for the (fictitious) fluid particles.

In order to model a two-phase fluid, we utilize the single-component multiphase model developed by Shan and Chen [20]. This model, as well as LB models in general, is well suited for porous-medium simulations as the solid boundaries are easily incorporated. It adopts an approach in which simple mesoscopic interactions are included in the model, and the macroscopic behavior of the system emerges from these interactions.

The Shan-Chen model has been successfully used in previous studies of multicomponent and multiphase flows in porous media [49,50]. In this model an attractive short-range interaction force

$$\mathbf{F}_G(\mathbf{r}) = -\psi(\mathbf{r})\sum_i G_i \psi(\mathbf{r} + \mathbf{c}_i)\mathbf{c}_i \tag{13}$$

is included between the (fictitious) fluid particles. Here $\psi(\mathbf{r}) = 1 - \exp[-\rho(\mathbf{r})]$ and $G_i = 2G$, G, or 0 for velocity vectors $\mathbf{c}_i$ of length $\sqrt{2}$, 1, or 0, respectively, and the parameter G is used to adjust the strength of the surface tension. This force gives rise to a spontaneous phase separation to liquid and vapor phases and to surface tension. Adhesive forces between fluid nodes and wall nodes are realized by adding a force

$$\mathbf{F}_W(\mathbf{r}) = -\psi(\mathbf{r})\sum_i W_i s(\mathbf{r} + \mathbf{c}_i)\mathbf{c}_i, \tag{14}$$

where $W_i = 2W$, W, or 0 for velocity vectors of length $\sqrt{2}$, 1, and 0, respectively, and $s = 0$ (1) if the node $\mathbf{r} + \mathbf{c}_i$ is a fluid (solid) node [49]. The parameter W is used to control the wettability of the liquid. These forces are included in the lattice-Boltzmann equation with a fluid velocity obtained from the first momentum of the distribution function at equilibrium,

$$\rho\mathbf{u} = \sum_i f_i(\mathbf{r},t)\mathbf{c}_i + \tau F_G + \tau F_W. \tag{15}$$

More sophisticated methods have also been developed for adding the forcing term in the LB method [51,52].

Notice, finally, that typical experiments include liquid (water) and air rather than liquid and vapor of that liquid. Therefore it would be more correct to use a multicomponent model (see, e.g., Refs. [19,20,53]) rather than a multiphase model in the simulations. The most important factors concerning the gas phase are, however, that it is in thermal and mechanical (local) equilibrium with the liquid phase—i.e., that its temperature and pressure are the same as those in the liquid phase in contact with it. To this end it is not important that the gas phase in our simulations is vapor of the liquid used. A possible effect that we cannot see in our simulations is entrapping of air bubbles in pores. We do not expect this effect to be important in the case of paper as air can quite freely move away from the advancing liquid front. Another problem that may arise from using a single-component multiphase model is a possible condensation of vapor. However, as we shall see in the next section, this problem is not significant in the present simulations as penetration of the liquid is "slow:" it happens through capillary forces without any external force. Furthermore, as there is no vapor reservoir in the system considered, the amount of material is much less in the vapor phase and its possible condensation cannot in principle produce a significant effect. Notice also that a two-component model would mean two sets of distribution functions, and this would lead to a significant increase in both the memory usage and the computational time needed.

IV. RESULTS

As already explained above, we simulated penetration of a wetting liquid in paper using a realistic three-dimensional x-ray tomographic reconstruction of a sample of paper board as the simulation geometry. The sample used was a hand sheet of a basis weight of 300 g/m^2, and the image used in the simulations was obtained with microtomographic techniques [54]. The porosity of the sample was 0.43, its specific surface area 1.68×10^5 m^2, and the typical fiber length about 2 mm. The image was $460 \times 460 \times 100$ lattice units, and its voxel size was approximately (2 μm)^3. Smaller subsamples were used in the simulations in order to keep the computational effort reasonable.

All simulations that are reported here were done using the relaxation-time parameter $\tau = 1.0$ and the values $G = -0.15$ and $W = -0.10$ for the cohesion and adhesion parameters, respectively. These values correspond to a surface tension of 0.85 (in lattice units) and a contact angle of 60°. The density difference between the liquid and vapor phases was about 20. Notice that the surface tension and contact angle cannot be directly deduced from the parameters of the model, but can be obtained numerically. The surface tension can be determined by simulating droplets of varying size and using then the Laplace law [20,49,55]. The contact angle can be deter-

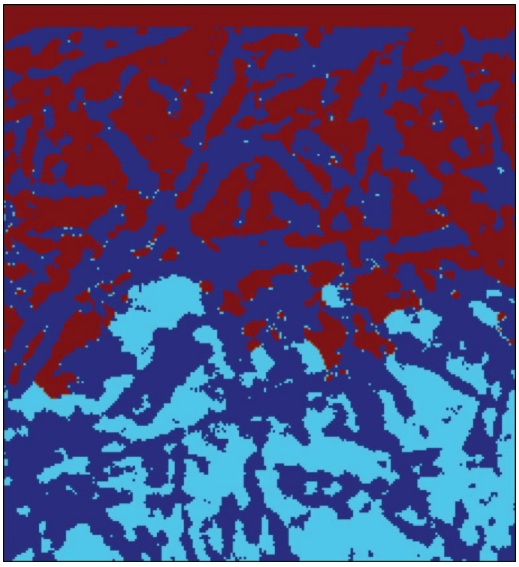

FIG. 1. (Color) Two-dimensional cross section of a unidirectional penetration of liquid. The liquid source is located at the upper boundary. Blue, red, and cyan are used for solid, liquid, and vapor phases, respectively.

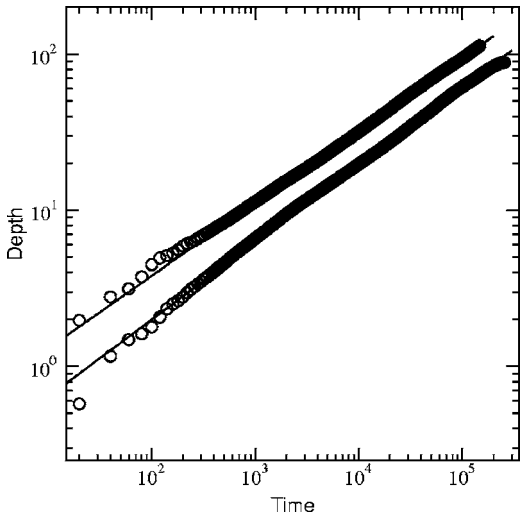

FIG. 2. Depth of the liquid front as a function of time for unidirectional penetration. The lower curve is for the transverse direction and the upper curve for the in-plane directions. Bending at the end of the lower simulated curve indicates that liquid had penetrated through the sample. Simulation results are marked with circles and Lucas-Washburn fits with solid lines. Results are given in dimensionless lattice units.

mined either from the shape of the droplet in contact with the solid material, which is typically not very reliable, or by using a suitable benchmark case such as the capillary tube simulation described below. Notice that the G and W parameters were chosen such that the capillary number was small—i.e., that capillary forces dominated over the inertial ones.

A. Unidirectional penetration

We first studied unidirectional penetration of liquid into the sample with an unlimited source of liquid (see Fig. 1). The liquid source was realized by imposing a pressure boundary condition [56] on one of the boundaries. Pressure was chosen such that the source did not cause any external force on the penetrating liquid. Therefore, liquid penetrated spontaneously into the sample because of capillary forces alone. Penetration was realized in the transverse direction as well as in the two in-plane directions of the sample. For these simulations, subsamples of sizes of $230\times230\times100$ and $230\times100\times460$ lattice units were used for penetration in the transverse and in-plane directions, respectively.

In Fig. 2 we show the location of the liquid front as a function of time. The location of the front was deduced from the total mass of the liquid penetrated in the system, as determination of the local front position would be rather inaccurate due to the fairly small penetration depths in the simulations. However, as we know the porosity of the sample and the densities of the liquid and vapor phases, a penetrated mass can easily be converted into a penetration depth. For the sake of clarity, results for only one of the in-plane directions are shown in Fig. 2, since the results for the other direction were almost the same. The Lucas-Washburn equation (3) describes well the results obtained even though the size of the sample is very small, of the order of one fiber length. Power-law fits to the time evolution of the simulation data gave the values 0.50, 0.47, and 0.47 (in the transverse and in-plane directions, respectively) for the scaling exponent, in good agreement with the Lucas-Washburn prediction 1/2.

Since all quantities in Eq. (3) are known except the contact angle and the tube radius, we can use the above power-law fits to determine an "effective capillary radius," $a_{eff} \equiv a\cos\theta$. In the transverse direction we obtained $a_{eff}=0.74$ μm and in the in-plane directions $a_{eff}=3.5$ μm and 2.8 μm. These values can be compared with the permeabilities obtained by single-phase LB simulations for the same sample [57]. As mentioned above, the permeability of a system that consists of capillary tubes of radius a can be calculated, and one finds that $k=\phi a^2/24$. Using this equation, capillary radii of 4.7 μm in the transverse direction and 6.2 μm and 6.4 μm in the in-plane directions are obtained from the permeability simulations. Direct comparison is difficult since the results of the Lucas-Washburn equation for a_{eff} should be divided by $\cos\theta$, which, however, is not known. To this end, we studied the rise of a column of the same liquid in a circular capillary tube in a gravitational field that was real-

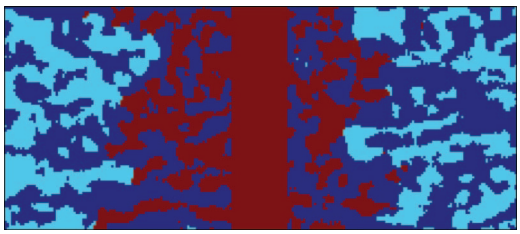

FIG. 3. (Color) Two-dimensional cross section of a radial penetration of liquid. The liquid source is located in the vertical hole in the middle of the sample. Colors are as in Fig. 1.

ized with a body force. After an equilibrium height for the liquid column was reached, a static contact angle was obtained from the equation

$$\cos\theta_s = \frac{z_\infty a g \Delta\rho}{2\gamma}, \tag{16}$$

where $\Delta\rho$ is the density difference between the liquid and vapor phases and z_∞ is the height of the column.

In practice the LB fluid is weakly compressible. The effect of compressibility was excluded by determining the factor $z_\infty\Delta\rho$ in Eq. (16) from a density integral along the center line of the tube and along a vertical line far from the tube.

For the parameters used in our simulations, we found that, in the static case, $\cos\theta \approx 0.5$. On the other hand, it is known that for a moving contact line the dynamic contact angle is larger than the static one (see, e.g., Refs. [58,59]). Taking these facts into account, we can conclude that the pore size obtained from our simulation agrees quite well with that obtained from permeability simulations. It is evident, however, that the results of single-phase and two-phase simulations for the transverse directions differ somewhat more than for the in-plane directions. This is most probably due to the simplified model we used for the permeability. For example, we did not take into account the tortuosity that can noticeably affect the permeability. For the paper-board sample used here, different tortuosities were indeed found for the transverse and in-plane directions [57]. Furthermore, the same tomographic image has also been analyzed by image analysis techniques [54] with a comparable result for the typical pore size in the system.

Notice that in experimental studies on samples of large size, the Lucas-Washburn equation has been found to correctly describe the penetration of liquid into paper [5,35,38].

B. Radial penetration

Let us consider two-dimensional radial penetration from an unlimited cylindrical reservoir of liquid. The geometrical setup of the simulation was the following: A cylindrical cavity was created across the sample in the transverse direction, and an unlimited source of liquid was placed in this cavity (cf. Fig. 3). Again, the pressure of the source was chosen such that penetration took place only due to capillary forces. The size of the sample in this simulation was $230\times230\times100$ lattice units.

We show in Fig. 4 the radius of the wetted area as a function of time. Again, instead of estimating the penetration radius from the location of the liquid front, we use an effective radius determined from the total amount of liquid penetrated into the system. Also shown in this figure is a fit by Eq. (8) of the simulation data, and an excellent agreement is found. From the fit, we can estimate an effective radius for the average capillary in the system, which in this case is 4.32 μm. This value is close to those obtained for unidirectional penetration, especially the ones in the in-plane directions.

In their experimental study on radial penetration of liquid from an unlimited reservoir, Danino and Marmur found that the time evolution of the squared radius of a wetted area could well be described by a power law, with an exponent varying between 0.85 and 0.88 [38]. In Fig. 5 we show in a log-log plot the effective radius squared of the wetted area as a function of time, as given by our simulation. It is evident that also these data can well be described by a power law, with an exponent in this case of 0.73. So far there is no explanation of the small deviation of this exponent from the experimental value of Danino and Marmur.

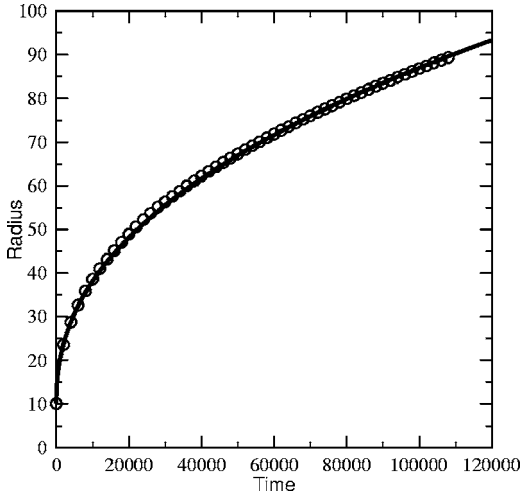

FIG. 4. Radial penetration of liquid. Simulation results (circles) are compared to Eq. (8) (solid line). Results are given in dimensionless lattice units.

C. Droplet penetration

Finally we studied the penetration of a small droplet into the same sample of paper board. In this simulation the size of the sample was $300\times300\times100$ lattice units, whereas the size of the whole simulation domain was $300\times300\times260$ lattice units, including a droplet with an initial diameter of about 95 lattice units. Initially the droplet was positioned just

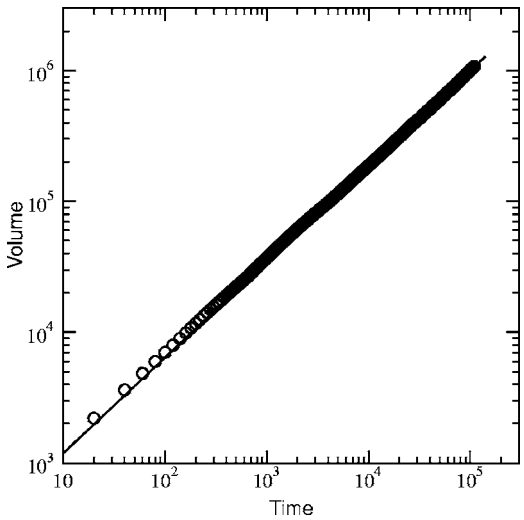

FIG. 5. Volume of penetrated liquid versus time in radial penetration. Circles mark simulation results and solid line a power-law fit to these results. Results are given in dimensionless lattice units.

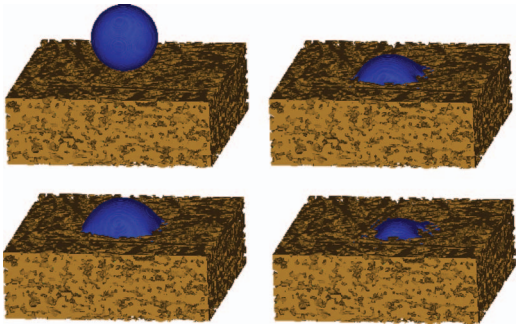

FIG. 6. (Color) Droplet penetration. Snapshots from four different stages of the penetration process.

above the sample surface and no initial velocity was given to it. Thus the Weber number (i.e., the ratio of the inertial and capillary forces) was small and no splashing of liquid occurred [60]. Capillary forces were then the only driving force that caused penetration of liquid into the sample.

Figure 6 shows the droplet at four different stages of penetration. To analyze the penetration kinetics, we measured the basal radius and the volume of the droplet above the sample surface as a function of time. The simulation result was compared with that obtained from the radial capillary model derived above. We used Eq. (6) such that it was integrated numerically, with R_0 in this case the time-dependent basal radius of the droplet. As is evident from Fig. 7, excellent qualitative agreement between this capillary model and the LB simulation was found. Notice that only those data related to capillary penetration were fitted by the capillary model. The mechanical phase, including oscillations of the droplet at the initial stages of the process, was excluded.

We observed a small discrepancy between the effective capillary radii for droplet penetration and unidirectional or radial penetration: For droplet penetration the effective capillary radius was 16.9 μm. There are several factors that may have contributed to this discrepancy. The droplet considered here was quite small. Typically, when penetration of droplets

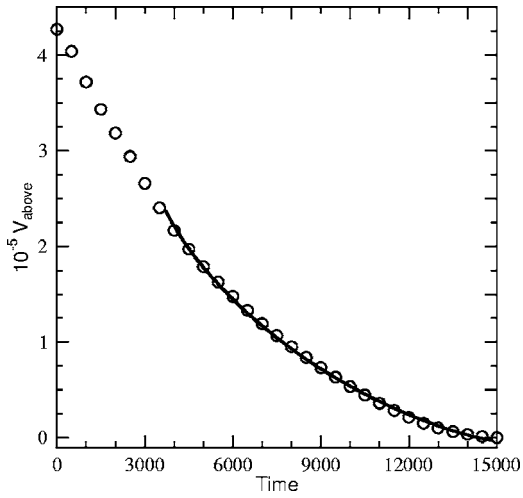

FIG. 7. Volume of liquid above the sample shown as a function of time. Simulation results (circles) are compared to the capillary model (solid line). Results are given in dimensionless lattice units.

into paper has been studied experimentally (see, e.g., Refs. [34,36–38]), the droplets used have been large enough so that the assumption of instantaneous saturation of the sample in the transverse direction has been reasonable. Although in our case the droplet penetrates not only in the in-plane directions but also in the transverse direction in the course of the simulation, we found that the liquid mostly stayed close to the initial surface. In other words, penetration in the transverse direction was much slower than in the in-plane directions.

This anisotropy in droplet penetration is similar to the one we found in unidirectional penetration, which was much slower in the transverse direction than in the in-plane directions. This means that the assumption of purely two-dimensional penetration in the vicinity of paper surface is not at all unreasonable, although penetration occurs also in the transverse direction. The small size of the droplet also means that the assumption of an unlimited source of liquid is not valid. In their experiments Borhan and Rungta [37] observed that the penetration of a large droplet could well be described by a capillary model with an unlimited source of liquid, at least qualitatively. What we have demonstrated above is that the penetration of a small droplet can also be described qualitatively by a rather similar model with, however, a rather obvious generalization that takes into account its finite size.

V. CONCLUSIONS

In conclusion, we studied penetration of a wetting liquid into a sample of paper board in three different situations using the LB method together with the Shan-Chen multiphase model. The sample used was a three-dimensional reconstruction of a real paper board obtained with high-resolution x-ray microtomography. We first simulated a unidirectional capillary penetration of liquid into the sample. In spite of the small size of the sample in comparison with the scale of structural heterogeneities of paper, our simulation results could be well described by the Lucas-Washburn equation, whose validity has previously been verified experimentally for large system sizes.

We then studied two-dimensional radial penetration of the liquid from an unlimited source. We demonstrated that in this case our simulation results could be explained with a radial capillary model. Thus, an appropriate capillary model was again able to describe the small-scale dynamics of the phenomenon. In this case as well as in the case of unidirectional penetration, the time evolution of the advancing liquid front followed a power law, albeit with a different scaling exponent. This exponent was 0.73 for radial penetration and 0.5 for unidirectional penetration.

Finally, we demonstrated the capability of the simulation method used to analyze the penetration of small droplets of liquid into paper. Furthermore, we showed that for this kind of penetration process, a generalized form of the radial capillary model described qualitatively the penetration dynamics. Basically one had to account for the fact that there is only a finite amount of liquid in the droplet. All these results indicate that somehow capillary type of models are more

general than expected on the basis of their simple assumptions concerning the pore structure. The simplified nature of the pore space of the material assumed in these capillary models means, however, that the effective pore size is, to some extent, a model-dependent parameter. Comparison of effective pore sizes can thus be made only at a qualitative level.

It would be of some interest to know how the leading front of the penetrating liquid proceeds in paper. For mainly technical reasons the quantitative properties of the front were difficult to determine. It was, however, evident that penetration was much faster along the plane of the sample than in the transverse direction. One could thus tentatively conclude that the leading front preferably proceeds along fibers, especially along contacts between two fibers, as then there is more liquid-solid interface available. In paper the fibers are mostly aligned in the planar directions.

In our simulations no swelling of the solid phase (fibers) due to the intruding liquid was present. Most of the experimental studies have also been done with such liquids that do not affect the fibers. One should, however, keep in mind that in many natural phenomena and technological processes, the penetrating liquid also enters the solid phase and causes its swelling while penetration proceeds in the pore network.

Our simulations show that the LB method together with the Shan-Chen multiphase model captures well the essential physics of capillary penetration. It has been reported previously in connection with a study of a single-capillary tube [59] that rather large tube radii are needed for a correct description of capillary rise. In the case of a porous material, the smallest pores are inevitably quite poorly discretized. We do not seem to find detectable effects related to this problem, however. Most probably the smallest pores give only a small contribution to the penetration process.

[1] R. Lucas, Kolloid-Z. **23**, 15 (1918).
[2] E. W. Washburn, Phys. Rev. **17**, 273 (1921).
[3] D. Quéré, Europhys. Lett. **39**, 533 (1997).
[4] B. V. Zhmud, F. Tiberg, and K. Hallstensson, J. Colloid Interface Sci. **228**, 263 (2000).
[5] J. Bico and D. Quéré, Europhys. Lett. **61**, 348 (2003).
[6] M. Alava, M. Dubé, and M. Rost, Adv. Phys. **53**, 83 (2004).
[7] M. A. Rubio, C. A. Edwards, A. Dougherty, and J. P. Gollub, Phys. Rev. Lett. **63**, 1685 (1989).
[8] S. V. Buldyrev, A.-L. Barabási, F. Caserta, S. Havlin, H. E. Stanley, and T. Vicsek, Phys. Rev. A **45**, R8313 (1992).
[9] L. A. N. Amaral, A.-L. Barabási, S. V. Buldyrev, S. Havlin, and H. E. Stanley, Phys. Rev. Lett. **72**, 641 (1994).
[10] O. Zik, T. Kustanovich, E. Moses, and Z. Olami, Phys. Rev. E **58**, 689 (1998).
[11] G. N. Constantinides and A. C. Payatakes, Transp. Porous Media **38**, 291 (2000).
[12] J. Bico, U. Thiele, and D. Quéré, Colloids Surf., A **206**, 41 (2002).
[13] D. H. Rothman and S. Zaleski, *Lattice-Gas Cellular Automata* (Cambridge University Press, Cambridge, England, 1997).
[14] S. Chen and G. D. Doolen, Annu. Rev. Fluid Mech. **30**, 329 (1998).
[15] S. Succi, *The Lattice Boltzmann Equation for Fluid Dynamics and Beyond* (Oxford University Press, Oxford, 2001).
[16] D. Yu, R. Mei, L.-S. Luo, and W. Shyy, Prog. Aerosp. Sci. **39**, 329 (2003).
[17] B. Ferréol and D. H. Rothman, Transp. Porous Media **20**, 3 (1995).
[18] A. Koponen, D. Kandhai, E. Hellén, M. Alava, A. Hoekstra, M. Kataja, K. Niskanen, P. Sloot, and J. Timonen, Phys. Rev. Lett. **80**, 716 (1998).
[19] A. K. Gunstensen, D. H. Rothman, S. Zaleski, and G. Zanetti, Phys. Rev. A **43**, 4320 (1991).
[20] X. Shan and H. Chen, Phys. Rev. E **47**, 1815 (1993); **49**, 2941 (1994).
[21] M. R. Swift, W. R. Osborn, and J. M. Yeomans, Phys. Rev. Lett. **75**, 830 (1995).
[22] A. D. Angelopoulos, V. N. Paunov, V. N. Burganos, and A. C. Payatakes, Phys. Rev. E **57**, 3237 (1998).
[23] X. He, S. Chen, and R. Zhang, J. Comput. Phys. **152**, 642 (1999).
[24] I. I. Bogdanov, V. V. Mourzenko, J.-F. Thovert, and P. M. Adler, Phys. Rev. E **68**, 026703 (2003).
[25] Z. Guo and T. S. Zhao, Phys. Rev. E **68**, 035302 (2003).
[26] A. J. C. Ladd and R. Verberg, J. Stat. Phys. **104**, 1191 (2001).
[27] S. Bekri and P. M. Adler, Int. J. Multiphase Flow **28**, 665 (2002).
[28] A. Shakib-Manesh, J. A. Åström, A. Koponen, P. Raiskinmäki and J. Timonen, Eur. Phys. J. E **9**, 97 (2002).
[29] P. Raiskinmäki, J. A. Åström, M. Kataja, M. Latva-Kokko, A. Koponen, A. Jäsberg, A. Shakib-Manesh, and J. Timonen, Phys. Rev. E **68**, 061403 (2003).
[30] J. Hyväluoma, P. Raiskinmäki, A. Koponen, M. Kataja, and J. Timonen, Phys. Rev. E **72**, 061402 (2005).
[31] G. Punzo, F. Massaioli, and S. Succi, Comput. Phys. **8**, 705 (1994).
[32] D. Kandhai, A. Koponen, A. G. Hoekstra, M. Kataja, J. Timonen, and P. M. A. Sloot, Comput. Phys. Commun. **111**, 14 (1998).
[33] J. Wang, X. Zhang, A. G. Bengough, and J. W. Crawford, Phys. Rev. E **72**, 016706 (2005).
[34] T. Gillespie, J. Colloid Sci. **13**, 32 (1958).
[35] R. Williams, J. Colloid Interface Sci. **79**, 287 (1981).
[36] E. Kissa, J. Colloid Interface Sci. **83**, 265 (1981).
[37] A. Borhan and K. K. Rungta, J. Colloid Interface Sci. **158**, 403 (1993).
[38] D. Danino and A. Marmur, J. Colloid Interface Sci. **166**, 245 (1994).
[39] F. Natterer, *The Mathematics of Computerized Tomography* (SIAM, Philadelphia, 2001).
[40] A. C. Kak and M. Slaney, *Principles of Computerized Tomographic Imaging* (SIAM, Philadelphia, 2001).
[41] R. Holmstad, Ph.D. thesis, Norwegian University of Science and Technology, 2004.
[42] E. J. Samuelsen, O. W. Gregersen, P. J. Houen, and T. Helle, J.

Pulp Pap. Sci. **27**, 50 (2001).
[43] T. Gureyev, R. Evans, A. W. Stevenson, D. Gao, and S. W. Wilkins, Tappi J. **84**, 52 (2001).
[44] A. Goel, M. Tzanankakis, S. Huang, S. Ramaswamy, D. Choi, and B. V. Ramarao, Tappi J. **84**, 1 (2001).
[45] G. W. Jackson and D. F. James, Can. J. Chem. Eng. **64**, 364 (1986).
[46] A. Marmur, J. Colloid Interface Sci. **124**, 301 (1988).
[47] P. L. Bhatnager, E. P. Gross, and M. Krook, Phys. Rev. **94**, 511 (1954).
[48] Y. H. Qian, D. d'Humières, and P. Lallemand, Europhys. Lett. **17**, 479 (1992).
[49] N. S. Martys and H. Chen, Phys. Rev. E **53**, 743 (1996).
[50] M. C. Sukop and D. Or, Physica B **338**, 298 (2003); Water Resour. Res. **40**, W01509 (2004).
[51] X. He, X. Shan, and G. D. Doolen, Phys. Rev. E **57**, R13 (1998).
[52] Z. Guo, C. Zheng, and B. Shi, Phys. Rev. E **65**, 046308 (2002).
[53] E. Orlandini, M. R. Swift, and J. M. Yeomans, Europhys. Lett. **32**, 463 (1995).
[54] S. Ramaswamy, S. Huang, A. Goel, A. Cooper, D. Choi, A. Bandyopadhyay, and B. V. Ramarao, in *Proceedings of the 12th Fundamental Research Symposium on the Science of Papermaking*, edited by C. F. Baker (Pulp and Paper Fundamental Research Society, Bury, Lancashire, UK, 2001), pp. 1289–1311.
[55] P. Raiskinmäki, A. Koponen, J. Merikoski, and J. Timonen, Comput. Mater. Sci. **18**, 7 (2000).
[56] Q. Zou and X. He, Phys. Fluids **9**, 1591 (1997).
[57] U. Aaltosalmi, M. Kataja, A. Koponen, J. Timonen, A. Goel, G. Lee, and S. Ramaswamy, J. Pulp Pap. Sci. **30**, 251 (2004).
[58] E. Schäffer and P. Z. Wong, Phys. Rev. E **61**, 5257 (2000).
[59] P. Raiskinmäki, A. Shakib-Manesh, A. Jäsberg, A. Koponen, J. Merikoski, and J. Timonen, J. Stat. Phys. **107**, 143 (2002).
[60] K. Range and F. Feuillebois, J. Colloid Interface Sci. **203**, 16 (1998).